Sensitivity Enhancement of Surface Plasmon Resonance Imaging Using Periodic Metallic Nanowires

Kyung Min Byun, Michael L. Shuler, Sung June Kim, Soon Joon Yoon, and Donghyun Kim

***Abstract*—A nanowire-mediated surface plasmon resonance (SPR) imaging is numerically investigated for enhanced sensitivity. The results calculated by rigorous coupled-wave analysis present that interplays between localized surface plasmons and surface plasmon polaritons contribute to sensitivity enhancement. Compared to conventional thin film-based SPR imaging measurement, an optimal nanowire structure can provide sensitivity enhancement by 3.44 times as well as highly linear detection property for quantification of surface reactions of interests. This paper demonstrates the potential and limitation for a highly sensitive, label-free, and real-time SPR imaging sensor based on periodic metallic nanowires.**

***Index Terms*—Imaging, metallic nanowires, optical sensors, sensitivity, surface plasmons.**

I. Introduction

SURFACE plasmon resonance (SPR) has been widely used in a variety of biosensors, since it provides rapid, label-free, and real-time sensing capability for monitoring biochemical interactions on a surface [1], [2]. Fluorescence-based biosensors have been developed quickly as well [3], [4]; however, they require complicated processes of binding fluorescent tags and have several disadvantages; for example, fluorescent proteins are expensive, time-consuming, and afflicted with lack of quantitative accuracy and photobleaching [5]. For these reasons, a surface-sensitive optical technique using SPR is used heavily for detection of bio-affinity interactions.

Manuscript received September 29, 2007; revised February 1, 2008. This work was supported by the International Collaboration Program, NBS-ERC (Nano Bioelectronics and Systems Research Center)/KOSEF (Korea Science and Engineering Foundation). The work of S. J. Yoon and D. Kim was supported by the Korea Science and Engineering Foundation (KOSEF) through National Core Research Center for Nanomedical Technology (R15-2004-024-00000-0) and KOSEF 2007-8-1158. Partial support was provided by a grant to the MEMS Research Center for National Defense funded by Defense Acquisition Program Administration under 2006-MM-41-5ND0600407. This work was also supported by the IT R&D program of MIC/IITA [2007-S001-01, Development of Implantable System Based on Biomedical Signal Processing], and by the "System IC 2010" project of Ministry of Knowledge Economy.

K. M. Byun was with the Department of Biomedical Engineering, Cornell University, Ithaca, NY 14853-5201 USA. He is now with the Department of Biomedical Engineering, Kyung Hee University, Yongin, Gyeonggi 449-701, Korea.

M. L. Shuler is with the Department of Biomedical Engineering, Cornell University, Ithaca, NY 14853-5201 USA.

S. J. Kim is with the School of Electrical Engineering and Computer Science, Seoul National University, Seoul 151-742, Korea.

S. J. Yoon and D. Kim are with the School of Electrical and Electronic Engineering, Yonsei University, Seoul 120-749, Korea (e-mail: kimd@yonsei.ac.kr).

Digital Object Identifier 10.1109/JLT.2008.922182

In recent years, with increasing demands for rapid measurement of a large number of samples, development of a high-throughput SPR microarray system has emerged as one of the most important SPR sensing applications. In general, three detection methods have been employed as an SPR imaging system, involving wavelength interrogation [6], angle interrogation [7], [8], and intensity measurement [9], [10]. Most of the relevant studies have employed intensity-based SPR imaging that measures reflectance changes caused by a slight variation in sensing layer thickness or refractive index on a sensor surface, largely because of the simplicity in structure without any moving component. For this reason, we will restrict our use of SPR imaging to an intensity-based system that captures SPR signals in images.

Regardless of the advantages of SPR imaging, however, intensity-based method suffers from relatively low detection accuracy because of insufficient sensitivity [11]. To overcome the restrictions on sensitivity, many interesting studies have been reported to enhance the sensitivity of SPR measurements. For instance, several phase detection methods have been developed using interferometry techniques [12], [13]. Though phase may produce more rapid changes than intensity, it has been found that interferometry-based phase detection systems tend to have small dynamic range and limitations in facilitating a real-time SPR array sensing [11]. On the other hand, colloidal metallic nanoparticles have been employed to amplify SPR signals. It was empirically reported that applying nanoparticles can enhance the sensitivity by more than an order compared to conventional SPR biosensors [14], [15]. Although resonant excitations of localized surface plasmon (LSP) modes using metallic nanoparticles result in large sensitivity enhancement [16], [17], this method is prone to application-specific process variations, thus inevitably accompanied by irreproducible sensitivity characteristics.

In this paper, we consider periodic metallic nanowires on a thin metal film as an alternative structure to improve sensitivity and reproducibility of SPR measurements. From our previous studies using a non-imaging angle interrogation type of SPR biosensors, the effect of nanowires was verified both theoretically and experimentally to enhance the sensitivity significantly [18], [19], [20], [21]. It is thus an obvious next step in an evolutionary path to investigate whether nanostructures such as periodic nanowires can equally enhance the sensitivity for SPR imaging.

Recently, an SPR imaging study using 2-D nanoposts was conducted at near-infrared (NIR) wavelength and showed the feasibility of sensitivity enhancement based on nanostructures, although truly high-throughput data in an array were not presented [22]. Experimental results showed that an optimal nanopost structure on a thin gold film provided fivefold SPR signal amplification. At long wavelengths, reflectance curves sharpen significantly so that a narrow SPR curve produces high sensing contrast and largely enhanced sensitivity [23], [24]. However, the use of NIR leads to a critical limitation for SPR microarray imaging. Since surface plasmon propagation length increases with wavelength, lateral image resolution of SPR imaging is significantly aggravated in NIR compared to visible wavelengths, which can be a concern in the case of imaging microscopy rather than high-throughput interaction analysis [24]. For example, the propagation length is about 2 μm at $\lambda = 633$ nm and 12 μm at $\lambda = 800$ nm for an SPR sensor using gold as supporting metal and water as an ambient medium [25].

In this paper, we investigate an enhanced SPR imaging structure based on periodic nanowires, in which excitations of and interactions with LSP modes are mediated by nanowires in the visible waveband. We intend to improve imaging resolution by employing visible waveband and simultaneously to achieve optimal sensor sensitivity for eventual microscopy applications. Design parameters of nanowires, such as nanowire period, size, and volume factor (VF) were optimized to obtain maximum sensitivity. In addition, extended analysis on linear sensing characteristics was performed for improved detection accuracy of nanowire-based SPR imaging measurements.

II. Numerical Models

For numerical analysis, rigorous coupled-wave analysis (RCWA) has been employed to calculate optical characteristics of periodic nanowires on a thin gold film [26], [27]. RCWA has been successfully applied to describing experiments with nanostructures [19], [28], [29]. Convergence was accomplished by including a sufficient number of spatial harmonic orders at the expense of prolonged computation [30].

A schematic diagram of a nanowire-mediated SPR imaging system is shown in Fig. 1. One-dimensional gold nanowires with a period Λ are assumed on a gold film with an attachment layer of chromium. The thicknesses of gold and chromium layers are fixed at 40 nm and 2 nm. Binding analytes are modeled as a 1-nm-thick self-assembled monolayer (SAM), which covers both gold nanowires and a gold film. We assumed 1,6-hexanedithiol (HDT) for the dielectric SAM by approximating it as a homogeneous layer with $n(HDT) = 1.52643$ [31]. A TM-polarized plane wave with fixed wavelength $\lambda = 633$ nm is used to illuminate one side of a prism/thin gold film sample at a predetermined incidence angle that produces a maximal intensity change. The reflectance change arises from the resonance shift created by changes in binding film thickness or refractive index at the sensor surface. The refractive index of an SF10 prism substrate and thin layers of chromium and gold were determined respectively as 1.723, $3.48 + 4.36i$, and $0.18 + 3.0i$ at $\lambda = 633$ nm [32]. The refractive index of a phosphate-buffered saline (PBS) solution was assumed to be 1.33. In particular, we estimated the effect of excited LSP modes by simplifying the profile of nanowires as a rectangle with width as $w_{\rm NW}$ and depth as $d_{\rm NW}$. The impact of more complicated nanowire geometries on SPR measurements was explored intensively in other studies [18], [33]. Here, a volume factor (VF) is introduced as $w_{\rm NF}/\Lambda$, which means the ratio of the volume occupied by gold nanowires. It is used to demonstrate that the nanowire width and period play an important role in improving SPR imaging detection characteristics.

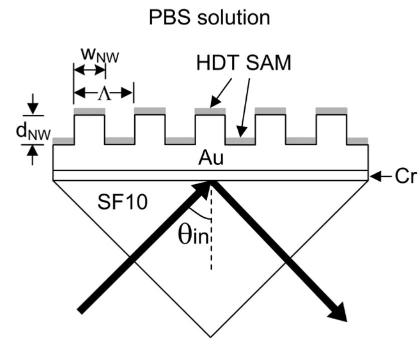

Fig. 1. Schematic diagram of a SPR imaging configuration with periodic gold nanowires. A TM-polarized light with $\lambda = 633$ nm is incident at an angle $\theta_{\rm in}$. A 40-nm-thick gold film is deposited on an SF10 prism substrate with an attachment chromium layer. Gold nanowires (period: Λ, width: $W_{\rm NW}$ and thickness: $d_{\rm NW}$) are regularly patterned on the gold film. Binding analytes are modeled as a 1-nm-thick HDT SAM in PBS so1ution.

A big difference in SPR imaging from our earlier investigations on non-imaging intensity-based SPR detection is that the quantitative measure of the sensitivity improvement in SPR imaging in reference to a conventional SPR imaging method is a reflectance sensitivity enhancement factor (RSEF) that is defined as

$$\text{RSEF}=\left|\frac{\Delta R_{\rm NWSPR}}{\Delta R_{\rm SPR}}\right| =\left|\frac{R_{\rm NWSPR}\,(\text{with analyte})-R_{\rm NWSPR}(\text{without analyte})}{R_{\rm SPR}(\text{with analyte})-R_{\rm SPR}(\text{without analyte})}\right| \tag{1}$$

where ΔR is the reflected intensity difference with binding analytes from without. Subscripts *NWSPR* and *SPR* represent a nanowire-enhanced and a conventional SPR imaging configuration.

III. Results and Discussion

Fig. 2 presents the reflectance characteristics versus incidence angle for conventional SPR detection without nanowires. The resonance angles with and without analytes are 59.94° and 59.75°; thus, the resonance shift is 0.19°. To determine a fixed incidence angle in SPR imaging measurements, we calculated the difference in SPR reflectance with and without analytes. It was found that the change in percent reflectance reaches a maximum of 3.41% ($\Delta R_{\rm SPR}$ in (1)) at 57.73°.

In Fig. 3, the SPR curves of a nanowire-mediated SPR configuration are shown when $\text{VF} = 0.1$ and nanowire period $\Lambda = 50$ nm. The resonance angle change is 1.05° with a maximum change at 11.42% in reflectance when $\theta_{\rm in} = 51.91°$. From the results of Figs. 2 and 3, angular sensitivity enhancement factor

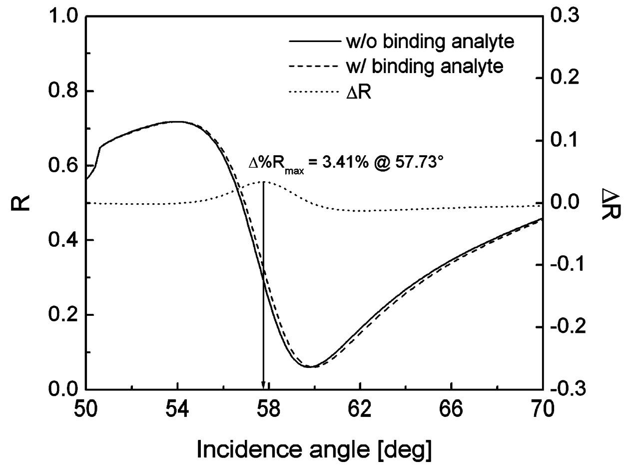

Fig. 2. SPR curves for a conventional SPR imaging structure. The dashed and solid lines represent with and without binding analytes and 4he resonance angles are 59.94° and 59.75°, respectively. The dotted curve is the difference (ΔR) between the SPR curves with and without analytes with a maximum at 3.41% at $\theta_{\rm in} = 57.73°$.

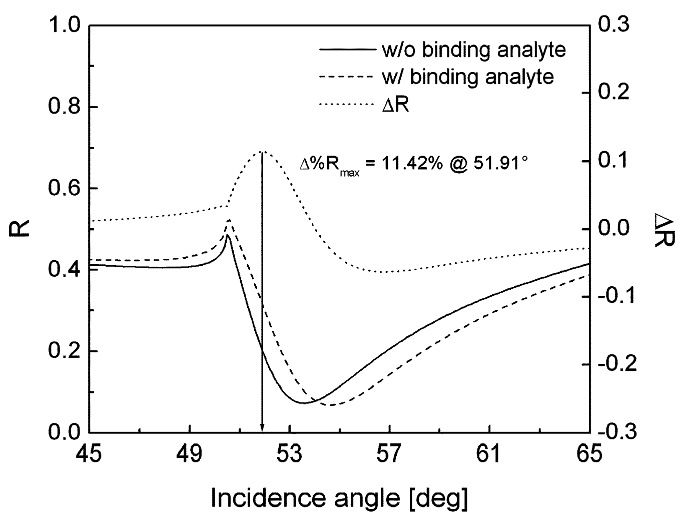

Fig. 3. SPR curves for a nanowire-mediated SPR imaging structuire at nanowire period $\Lambda = 50$ nm, $VF = 0.1$, and $d_{\rm Nw} = 20$ nm. The dashed and solid lines represent with and without binding analytes with resonance angles at 54.63° and 53.58°, respectively. The dotted curve is the difference (ΔR) between the SPR curves with and without analytes with a maximum at 41.42% at $\theta_{\rm in} = 51.91°$.

(ASEF) [18] and RSEF were determined to be 5.53 and 3.35, respectively. Note that reflectance amplitude and SPR angular curve width have been affected by the presence of nanowires. These parameters can be employed to explaining the relation between ASEF and RSEF, which is to be discussed in more detail subsequently.

Using (1), the impact of nanowire period ($\Lambda = 50$, 100, and 200 nm) on RSEF at various VFs was investigated when nanowire depth is fixed at 20 nm. For one-dimensional nanowires, a VF is equivalent to a fill factor or a volume concentration of nanowires. The resolution of VF was determined to ensure validation of RCWA method, such that the nanowire feature size is larger than $10\lambda_F$, where λ_F denotes the Fermi wavelength and is approximately 0.5 nm for gold.

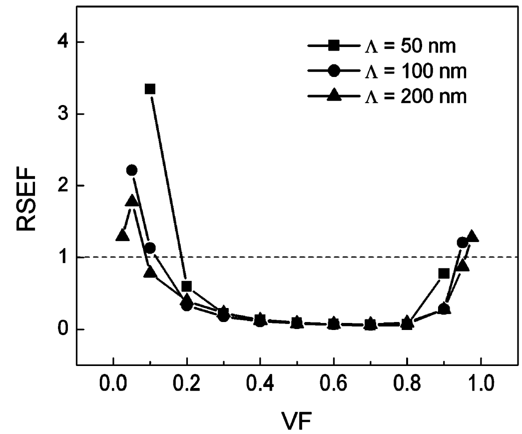

Fig. 4. RSEF characteristics with VF for nanowires at $\Lambda = 50$ nm (squares), 100 nm (circles), and 200 nm (triangles). VF varies from 0 to 1. The dotted line presents the relative sensitivity based on reflectance for a conventional SPR imaging structure.

First of all, Fig. 4 shows that for all the nanowire periods, RSEF can be enhanced when $w_{\rm NW} < 10$ nm (for VF values near $\rm VF = 0$) and a gap between nanowires is less than 5 nm (for VF values near $\rm VF = 1$). At small VFs that give rise to improved RSEFs, a coupling effect between surface plasmon polaritons (SPPs) excited on a bulk gold film and LSPs in nanowires is more dominant than coupling of LSPs, because the structural perturbation is not significant compared to a bulk SPR structure with 40-nm or 60-nm thickness and propagating SPPs are still efficient. The enhancement near $\rm VF = 0$ is associated with the interaction between SPPs and strong excitations of LSPs in an individual nanowire. LSP resonance (LSPR) excitation in a single nanostructure has been known to be strong enough to analyze a small amount of biomolecular binding events [34]. On the other hand, at high VF values, extreme plasmon couplings between SPPs and LSPs on a gold surface through nanogrooves are attributed to the enhanced sensitivity, though it is less effective than RSEF at low VF values. Electromagnetic field enhancement by near-field interactions typically generates hot spots around nano-sized metallic structures [35], [36] and also leads to a significant sensitivity gain [37]. Especially, in hot spots with a gap size smaller than 10 nm, the local fields can be enhanced up to more than 10^3 times of the incident field intensity [38], [39]. Calculations using finite-difference time domain method, though not shown, confirm that nonoverlapping and inefficient interactions between highly excited LSPs and a target SAM layer at high VFs result in a smaller RSEF than the enhancement that would be due only to hot spots. Also note that physics of coupling mechanisms and their impact on sensitivity enhancement were discussed using dispersion relation in terms of effective media in [40].

Second, for the values of VFs ranging from 0.2 to 0.9, RSEF is calculated to be much lower than the dotted line, indicating the relative sensitivity of a conventional SPR imaging detection method. In this region, a higher VF generally produces stronger LSPR and LSPs are more dominantly excited than SPPs, since a larger nanowire volume and a smaller nanowire separation induce stronger interactions between neighboring LSP modes.

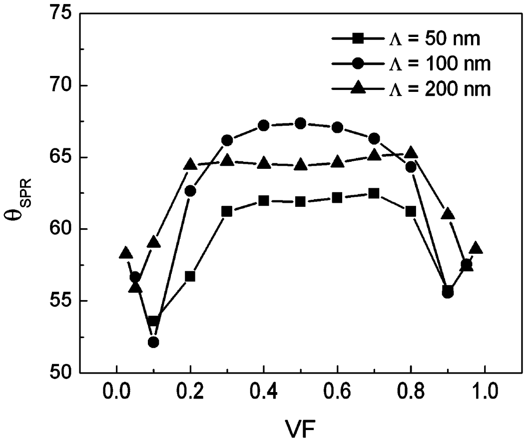

Fig. 5. Resonance angles with VF for nanowires at $\Lambda = 50$ nm (squares), 100 nm (circles), and 200 nm (triangles).

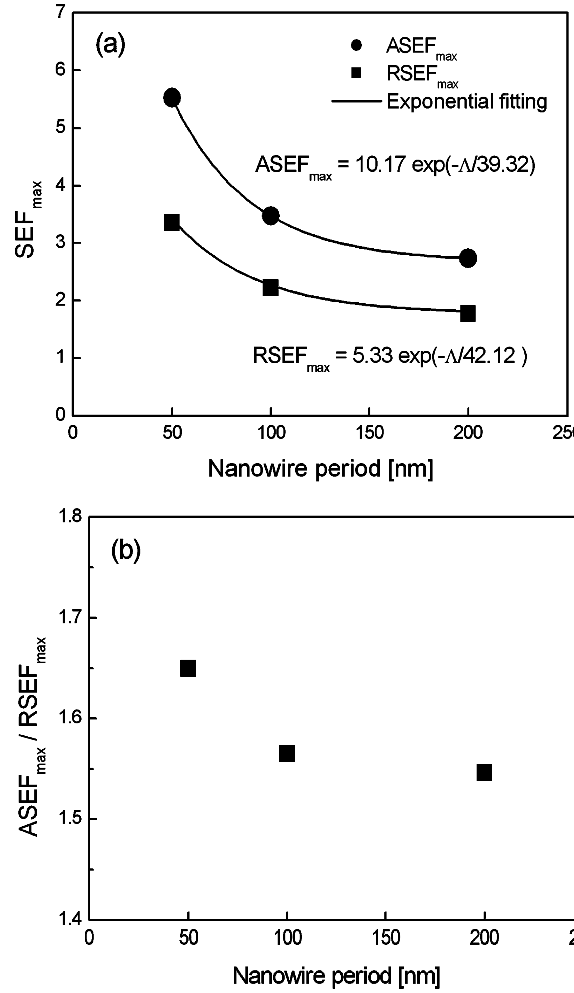

Fig. 6. (a) Peak SEF plots with nanowire period ranging from 50 nm to 200 nm. The peak SEFs are obtained to be 5.53 ($\Lambda = 50$ nm), 3.47 ($\Lambda = 100$ nm), and 2.74 ($\Lambda = 200$ nm) for ASEF (circles), and 3.35 ($\Lambda = 50$ nm), 2.22 ($\Lambda = 100$ nm), and 1.77 ($\Lambda = 200$ nm) for RSEF (squares), respectively. The is solid line is an exponential fit. (b) The ratio of $\mathrm{ASEF_{max}}$ to $\mathrm{RSEF_{max}}$ with nanowire period. The ratio is equal to 1.650 ($\Lambda = 50$ nm), 1.565 ($\Lambda = 100$ nm), and 1.546 ($\Lambda = 200$ nm).

However, because the reflectance amplitude and the SPR curve width are affected by the presence of nanowires, LSPR enhancement and an improved RSEF may not be positively correlated at all times, in contrast to the results observed with angle-scanning nanowire-based LSPR. As shown in Fig. 5, strongly excited LSP modes occur at an increased resonance angle of $\theta_{\mathrm{SPR}} > 60°$. This indicates that the perturbation introduced by the nanowires modifies strongly the SPPs in the gold film. In other words, the momentum matching is achieved at a higher wave-number, and thus much higher energy is needed to excite a LSP mode. Moreover, LSPR enhancement is essentially accompanied by the broadening of an SPR curve in conjunction with the LSP perturbation and deterioration of sensing contrast of SPR detection due to the damping into a large number of LSP modes [39], [41]. Here, the sensing contrast may be loosely defined as $(R_{\max} - R_{\min})/(R_{\max} + R_{\min})$, where $R_{\max}$ is the reflectance at total internal reflection, and $R_{\min}$ is the minimum reflectance at resonance. As a result, dominantly excited LSP modes in nanowires lead to a larger resonance angle, a broader SPR curve, and lower sensing contrast, and eventually result in substantial reduction of RSEF compared with conventional SPR imaging.

Third, the results of Fig. 4 present the sensitivity improvement with a decrease in Λ. The peak RSEF was found to be 3.35 at $\mathrm{VF} = 0.1$ for $\Lambda = 50$ nm, 2.22 at $\mathrm{VF} = 0.05$ for $\Lambda = 100$ nm, and 1.77 at $\mathrm{VF} = 0.05$ for $\Lambda = 200$ nm, respectively. As Λ decreases, the surface number density of nanowires becomes larger, and this can induce stronger coupling between LSPs. Intensity amplification of LSPs can increase interactions with SPPs and, thus, produce a notable increment of maximum ASEF and RSEF, as presented in Fig. 6(a). The distribution of $\mathrm{SEF_{max}}$ values and its exponential fit are well matched for both ASEF and RSEF. Using the first-order exponential function of $y = y_0 \exp(-kx)$, the integration constant (y_0) and the exponential coefficient (k) are equal to 10.17 and $0.02543 (= 1/39.32)$ for $\mathrm{ASEF_{max}}$, and 5.33 and $0.02374 (= 1/42.12)$ for $\mathrm{RSEF_{max}}$. That $k\ (\mathrm{ASEF_{max}}) \approx k\ (\mathrm{RSEF_{max}})$ implies the similarity of the overall behavior of $\mathrm{ASEF_{max}}$ and $\mathrm{RSEF_{max}}$ with respect to nanowire period.

It is interesting to note that, in general, $\mathrm{RSEF_{max}}$ is smaller than $\mathrm{ASEF_{max}}$. This is because the reflectance change as a result of an SPR shift is accompanied by resonance broadening and reduced sensing contrast, which tends to decrease the reflectance change. In other words, the decrease of differential reflectance, which corresponds to the slope of an SPR curve near the resonance angle, leads to a reduced reflectance change. It is also found from the exponential coefficients of exponential fits that $\mathrm{ASEF_{max}}$ increases slightly faster than $\mathrm{RSEF_{max}}$ with a decrease in Λ. Since excited LSP modes are strongly influenced with a decrease of Λ, the broadening of the SPR characteristics can evoke a moderate increase of $\mathrm{RSEF_{max}}$, and this in turn produces an increase in the ratio between the two peak values of ASEF and RSEF, i.e., $\mathrm{ASEF_{max}}/\mathrm{RSEF_{max}}$ [see Fig. 6(b)].

The dependence of RSEF on d_{NW} was investigated to further optimize the sensitivity of nanowire-mediated SPR imaging detection for various combinations of Λ and VF. The combinations were determined to provide maximum RSEF (shown in Fig. 4). In general, if LSPs perturb SPPs weakly in shallow nanowires, i.e., LSPs are dominated by SPPs, local field enhancement and sensitivity improvement over conventional SPR structure is rather weak. On the other hand, if LSPs dominate

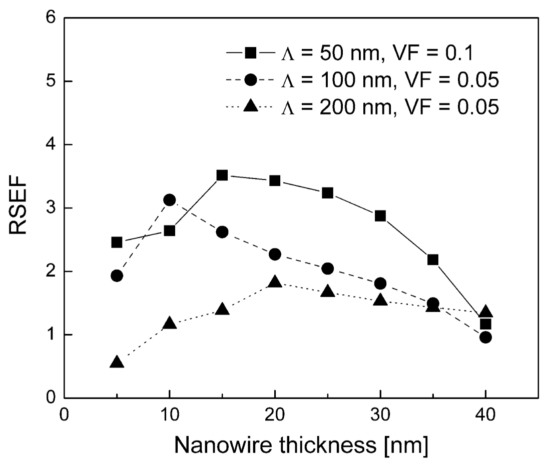

Fig. 7. RSEF characteristics with nanowire thickness $d_{\rm NW}$ varying from 5 nm to 40 nm with a step of 5 nm. The RSEF reaches a maximum of 3.44 at $d_{\rm NW} = 15$ nm for $\Lambda = 50$ nm (squares), 3.05 at $d_{\rm NW}$ 10 nm for $\Lambda = 100$ nm (circles), and 1.77 at $d_{\rm NW} = 20$ nm for $\Lambda = 200$ nm (triangles).

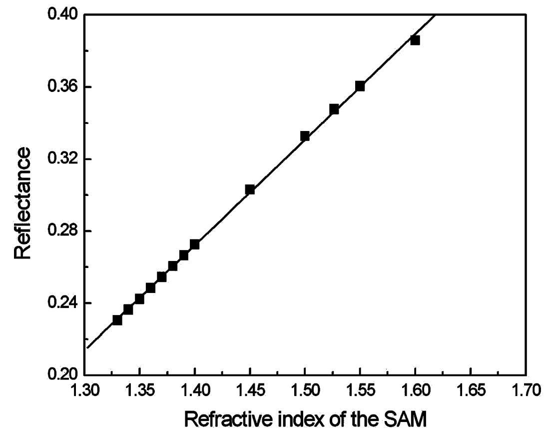

Fig. 8. Linear regression analysis between reflectance and refractive index of a 1-nm-thick SAM in PBS solution. As the refractive index increases from 1.33 to 1.60, the percent reflectance shifts from 23.05% to 38.59% linearly. The correlation coefficient R is equal to 0 99966.

TABLE I
CALCULATION RESULTS OF THE OPTIMIZED NANOWIRE STRUCTURE AT EACH NANOWIRE PERIOD

	Λ = 50 nm VF = 0.1	Λ = 100 nm VF = 0.05	Λ = 200 nm VF = 0.05
d_{NW} [nm]	15	10	20
RSEF	3.44	3.05	1.77
θ_{in} [deg]	51.86	54.18	53.49

SPPs in thick nanowires, resonance characteristics tend to be so broad that resonance can effectively disappear. Thus, an optimum nanowire depth exists as Fig. 7 shows, although the optimum may depend on other parameters. In Fig. 7, RSEF characteristics were calculated for $d_{\rm NW} = 5 - 40$ nm with a step of 5 nm. Table I summarizes the optimal structures of nanowires and its RSEF. The optimized nanowire structure is $\Lambda = 50$ nm, $w_{\rm NW} = 5$ nm $({\rm VF} = 0.1)$, and $d_{\rm NW} = 15$ nm with the highest RSEF obtained as 3.44 at $\theta_{\rm in} = 51.86^\circ$.

For nanowire-mediated SPR imaging detection to be useful quantitatively, it is important that changes of reflectance be linearly proportional to changes of refractive index on a sensor surface, and thus to the amount of bound analytes. Based on an assumption that the refractive index of 1-nm-thick SAM layer changes from 1.33, i.e., without a SAM in PBS solution, to 1.60 in accordance with the concentration of adsorbed analytes, Fig. 8 shows the calculated change in reflectance intensity at a fixed incidence angle of $\theta_{\rm in} = 51.86^\circ$ when an optimal nanowire structure with $\Lambda = 50$ nm, $d_{\rm NW} = 15$ nm, and $w_{\rm NW} = 5$ nm is employed on a 40-nm-thick gold film. For a broad range of percent reflectance of more than 10%, a linear relationship over the whole range of refractive indices is evident. From linear regression analyses, the change of reflectance was extremely linear with $R = 0.99966$ (R is the correlation coefficient that denotes the linearity obtainable in the sensor performance). This indicates that the application of nanowires enables large and highly linear dynamic range as well as enhanced sensitivity for an intensity-based SPR imaging system.

Finally, an interesting possibility is to employ a dielectric spacer layer below nanowires in order to modulate local plasmonic fields thereby sensitivity. Although details will be addressed in a subsequent study, the presence of a spacer layer was found to affect the interaction between LSPs and propagating SPs [42].

In regard to actual implementation, periodic gold nanowires on a gold film can be fabricated using electron-beam lithography or nanoimprinting techniques as reported recently [43], [44], although achieving high aspect ratio in a reproducible manner still remains a challenge. The relevant fabrication work is currently under way with the attachment of a SAM using 11-mercaptoundecylamine in a real-time multichannel fluidic system.

IV. CONCLUSION

We studied the impact of periodic nanowires on the sensitivity enhancement in SPR imaging biosensors using RCWA. Compared with conventional SPR imaging detection, periodic gold nanowires on a gold film lead to large SPR signal amplification due to the excitations and coupling of bulk SPPs and LSPs in gold nanowires. We found that periodic nanowires with narrow width and small period present enhanced sensitivity in terms of RSEF. It was also shown that $\text{RSEF}_{\max}$ is generally less than $\text{ASEF}_{\max}$, since RSEF is strongly influenced by the broadening of a SPR curve and a decrease of sensing contrast, accompanied by the presence of nanowires.

The peak RSEF achieved was 3.44 with nanowires of a rectangular profile at $\Lambda = 50$ nm, $w_{\rm NW} = 5$ nm, and $d_{\rm NW} = 15$ nm. For this optimum structure, the results calculated in PBS solution present extremely linear sensing characteristics over a broad range of binding refractive index. Our study on a nanowire-mediated SPR imaging system demonstrates the possibility of sensitivity improvement and a potential to implement a rapid real-time SPR microarray imaging system with enhanced sensitivity.

REFERENCES

[1] B. Rothenhäusler and W. Knoll, "Surface-plasmon microscopy," *Nature*, vol. 332, pp. 615–617, Apr. 1988.

[2] J. Homola, S. S. Yee, and G. Gauglitz, "Surface plasmon resonance sensors: Review," *Sens. Actuators B*, vol. 54, no. 1, pp. 3–15, Jan. 1999.

[3] K. L. Prime and G. M. Whitesides, "Self-assembled organic monolayers: Model systems for studying adsorption of proteins at surfaces," *Science*, vol. 252, no. 5010, pp. 1164–1167, May 1991.

[4] P. Mitchell, "A perspective on protein microarrays," *Nat. Biotechnol.*, vol. 20, no. 3, pp. 225–229, Mar. 2002.

[5] C. L. Wong, H. P. Ho, T. T. Yu, Y. K. Suen, W. W. Y. Chow, S. Y. Wu, W. C. Law, W. Yuan, W. J. Li, S. K. Kong, and C. Lin, "Two-dimensional biosensor arrays based on surface plasmon resonance phase imaging," *Appl. Opt.*, vol. 46, no. 12, pp. 2325–2332, Apr. 2007.

[6] J. Homola, "Present and future of surface plasmon resonance biosensors," *Anal. Bioanal. Chem.*, vol. 377, no. 3, pp. 528–539, Oct. 2003.

[7] C. E. Jordan, A. G. Frutos, A. J. Thiel, and R. M. Corn, "Surface plasmon resonance imaging measurements of DNA hybridization adsorption and streptavidin/DNA multilayer formation at chemically modified gold surfaces," *Anal. Chem.*, vol. 69, no. 24, pp. 4939–4947, Dec. 1997.

[8] N. Bassil, E. Maillart, M. Canva, Y. Levy, M.-C. Millot, S. Pissard, R. Narwa, and M. Goossens, "One hundred spots parallel monitoring of DNA interactions by SPR imaging of polymer-functionalized surfaces applied to the detection of cystic fibrosis mutations," *Sens. Actuators B*, vol. 94, no. 3, pp. 313–323, Oct. 2003.

[9] P. Guedon, T. Livache, F. Martin, F. Lesbre, A. Roget, G. Bidan, and Y. Levy, "Characterization and optimization of a real-time, parallel, label-free, polypyrrole-based DNA sensor by surface plasmon resonance imaging," *Anal. Chem.*, vol. 72, no. 24, pp. 6003–6009, Nov. 2000.

[10] H. J. Lee, T. T. Goodrich, and R. M. Corn, "SPR imaging measurement of 1D and 2D DNA micro-arrays created from microfluidic channels on gold thin films," *Anal. Chem.*, vol. 73, no. 22, pp. 5525–5531, Nov. 2001.

[11] Y. Xinglong, W. Dingxin, W. Xing, D. Xiang, L. Wei, and Z. Xinsheng, "A surface plasmon resonance imaging interferometry for protein micro-array detection," *Sens. Actuators B*, vol. 108, no. 1–2, pp. 765–771, Jul. 2005.

[12] C.-M. Wu, Z.-C. Jian, S.-F. Joe, and L.-B. Chang, "High-sensitivity sensor based on surface plasmon resonance and heterodyne interferometry," *Sens. Actuators B*, vol. 92, no. 1–2, pp. 133–136, Jul. 2003.

[13] H. P. Ho and W. W. Lam, "Application of differential phase measurement technique to surface plasmon resonance sensors," *Sens. Actuators B*, vol. 96, no. 3, pp. 554–559, Dec. 2003.

[14] L. He, M. D. Musick, S. R. Nicewarner, F. G. Salinas, S. J. Benkovic, M. J. Natan, and C. D. Keating, "Colloidal Au-enhanced surface plasmon resonance for ultrasensitive detection of DNA hybridization," *J. Amer. Chem. Soc.*, vol. 122, no. 38, pp. 9071–9077, Sep. 2000.

[15] L. A. Lyon, M. D. Musick, and M. J. Natan, "Colloidal Au-enhanced surface plasmon resonance immunosensing," *Anal. Chem.*, vol. 70, no. 24, pp. 5177–5183, Nov. 1998.

[16] T. Okamoto, I. Yamaguchi, and T. Kobayashi, "Local plasmon sensor with gold colloid monolayers deposited upon glass substrates," *Opt. Lett.*, vol. 25, no. 6, pp. 372–374, Mar. 2000.

[17] E. Hutter and J. H. Fendler, "Exploitation of localized surface plasmon resonance," *Adv. Mater.*, vol. 16, no. 19, pp. 1685–1706, Oct. 2004.

[18] K. M. Byun, S. J. Kim, and D. Kim, "Design study of highly sensitive nanowire-enhanced surface plasmon resonance biosensors using rigorous coupled wave analysis," *Opt. Express*, vol. 13, no. 10, pp. 3737–3742, May 2005.

[19] K. M. Byun, S. J. Yoon, D. Kim, and S. J. Kim, "Experimental study of sensitivity enhancement in surface plasmon resonance biosensors by use of periodic metallic nanowires," *Opt. Lett.*, vol. 32, no. 13, pp. 1902–1904, Jul. 2007.

[20] K. Kim, S. J. Yoon, and D. Kim, "Nanowire-based enhancement of localized surface plasmon resonance for highly sensitive detection: A theoretical study," *Opt. Express*, vol. 14, no. 25, pp. 12419–12431, Dec. 2006.

[21] S. J. Yoon and D. Kim, "Target dependence of the sensitivity in periodic nanowire-based localized surface plasmon resonance biosensors," *J. Opt. Soc. Amer. A*, vol. 25, no. 3, pp. 725–735, Mar. 2008.

[22] L. Malic, B. Cui, T. Veres, and M. Tabrizian, "Enhanced surface plasmon resonance imaging detection of DNA hybridization on periodic gold nanoposts," *Opt. Lett.*, vol. 32, no. 21, pp. 3092–3094, Nov. 2007.

[23] A. Ikehata, X. Li, T. Itoh, Y. Ozaki, and J.-H. Jiang, "High sensitive detection of near-infrared absorption by surface plasmon resonance," *Appl. Phys. Lett.*, vol. 83, no. 11, pp. 2232–2234, Sep. 2003.

[24] B. P. Nelson, A. G. Frutos, J. M. Brockman, and R. M. Corn, "Near-infrared surface plasmon resonance measurements of ultrathin films. 1. Angle shift and SPR imaging experiments," *Anal. Chem.*, vol. 71, no. 18, pp. 3928–3934, Aug. 1999.

[25] K. Johansen, H. Arwin, I. Lundström, and B. Liedberg, "Imaging surface plasmon resonance sensor based on multiple wavelengths: Sensitivity considerations," *Rev. Sci. Instrum.*, vol. 71, no. 9, pp. 3530–3538, Sep. 2000.

[26] M. G. Moharam and T. K. Gaylord, "Diffraction analysis of dielectric surface-relief gratings," *J. Opt. Soc. Amer.*, vol. 72, no. 10, pp. 1385–1392, Oct. 1982.

[27] M. G. Moharam and T. K. Gaylord, "Rigorous coupled-wave analysis of metallic surface-relief gratings," *J. Opt. Soc. Amer. A*, vol. 3, pp. 1780–1787, Nov. 1986.

[28] J. Cesario, R. Quidant, G. Badenes, and S. Enoch, "Electromagnetic coupling between a metal nanoparticle grating and a metallic surface," *Opt. Lett.*, vol. 30, no. 24, pp. 3404–3406, Dec. 2005.

[29] Y. Kanamori, K. Hane, H. Sai, and H. Yugami, "100 nm period silicon antireflection structures fabricated using a porous alumina membrane mask," *Appl. Phys. Lett.*, vol. 78, no. 2, pp. 142–143, Jan. 2001.

[30] L. Li and C. W. Haggans, "Convergence of the coupled-wave method for metallic lamellar diffraction gratings," *J. Opt. Soc. Amer. A*, vol. 10, no. 6, pp. 1184–1189, Jun. 1993.

[31] E. Hutter, S. Cha, J.-F. Liu, J. Park, J. Yi, J. H. Fendler, and D. Roy, "Role of substrate metal in gold nanoparticle enhanced surface plasmon resonance imaging," *J. Phys. Chem. B*, vol. 105, no. 1, pp. 8–12, Jan. 2001.

[32] E. D. Palik, *Handbook of Optical Constants of Solids*. Orlando, FL: Academic, 1985.

[33] J. P. Kottmann and O. J. F. Martin, "Influence of the cross section and the permittivity on the plasmon-resonance spectrum of silver nanowires," *Appl. Phys. B*, vol. 73, no. 4, pp. 299–304, Sep. 2001.

[34] G. Raschke, S. Kowarik, T. Franzl, C. Sönnichsen, T. A. Klar, J. Feldmann, A. Nichtl, and K. Kürzinger, "Biomolecular recognition based on single gold nanoparticle light scattering," *Nano Lett.*, vol. 3, no. 7, pp. 935–938, May 2003.

[35] L. Qin, S. Zou, C. Xue, A. Atkinson, G. C. Schatz, and C. A. Mirkin, "Designing, fabricating, and imaging Raman hot spots," *Proc. Nat. Acad. Sci.*, vol. 103, no. 36, pp. 13300–13303, Sep. 2006.

[36] E. Hao and G. C. Schatz, "Electromagnetic fields around silver nanoparticles and dimers," *J. Chem. Phys.*, vol. 120, no. 1, pp. 357–366, Jan. 2004.

[37] L. A. Lyon, D. J. Pena, and M. J. Natan, "Surface plasmon resonance of Au colloid-modified Au films: Particle size dependence," *J. Phys. Chem. B*, vol. 103, no. 28, pp. 5826–5831, Jun. 1999.

[38] H. Wang, C. S. Levin, and N. J. Halas, "Nanosphere arrays with controlled sub-10-nm gaps as surface-enhanced Raman spectroscopy substrates," *J. Amer. Chem. Soc.*, vol. 127, no. 43, pp. 14992–14993, Oct. 2005.

[39] C. L. Haynes, A. D. McFarland, and R. P. v. Duyne, "Surface-enhanced Raman spectroscopy," *Anal. Chem.*, vol. 77, pp. 338A–346A, 2005.

[40] D. Kim, "Effect of resonant localized plasmon coupling on the sensitivity enhancement of nanowire-based surface plasmon resonance biosensors," *J. Opt. Soc. Amer. A*, vol. 23, no. 9, pp. 2307–2314, Sep. 2006.

[41] K. M. Byun, D. Kim, and S. J. Kim, "Investigation of the profile effect on the sensitivity enhancement of nanowire-mediated localized surface plasmon resonance biosensors," *Sens. Actuators B*, vol. 117, no. 2, pp. 401–407, Oct. 2006.

[42] W. R. Holland and D. G. Hall, "Surface-plasmon dispersion relation: Shifts induced by the interaction with localized plasma resonances," *Phys. Rev. B*, vol. 27, no. 12, pp. 7765–7768, Jun. 1983.

[43] K. Yamazaki and H. Namatsu, "5-nm-order electron-beam lithography for nanodevice fabrication," *Jpn. J. Appl. Phys.*, vol. 43, no. 6B, pp. 3767–3771, Jun. 2004.

[44] M. D. Austin, H. Ge, W. Wu, M. Li, Z. Yu, D. Wasserman, S. A. Lyon, and S. Y. Chou, "Fabrication of 5 nm linewidth and 14 nm pitch features by nanoimprint lithography," *Appl. Phys. Lett.*, vol. 84, no. 26, pp. 5299–5301, Jun. 2004.

Kyung Min Byun received the B.S. and M.S. degrees from the School of Electrical Engineering, Seoul National University, Seoul, Korea, and the Ph.D. degree from Seoul National University, in 2007.

From July 2007 to February 2008, he worked as a Visiting Scientist in the Department of Biomedical Engineering, Cornell University, Ithaca, NY. He is currently an Assistant Professor at the Department of Biomedical Engineering, Kyung Hee University, Gyeonggi, Korea. His main research activities are theoretical and experimental studies on highly sensitive localized SPR biosensors with metallic nanostructures and SPR imaging microarray systems.

Michael L. Shuler received the B.S. degree from the University of Notre Dame, Notre Dame, IN, in 1969 and the Ph.D. degree in chemical engineering from University of Minnesota, Minneapolis, in 1973.

He has been a member of the Cornell University, Ithaca, NY, faculty since 1974 and has earned two teaching awards. He is on the editorial boards of four scientific journals. His research focuses on applying chemical reaction engineering principles to biological systems and he is also investigating targeted drug delivery to multidrug-resistant cancer cells.

Prof. Shuler is a Fellow of the American Institute of Medical and Biological Engineers for which he has served as Vice President for education. He has received the Amgen Award in biochemical engineering and was elected to membership in the National Academy of Engineers and the American Academy of Arts and Sciences.

Sung June Kim received the B.S. degree in electronics engineering from Seoul National University, Seoul, Korea, in 1978 and the M.S. and Ph.D. degrees from Cornell University, Ithaca, NY, in 1981 and 1983, respectively.

He was with the AT&T Bell Laboratories as a member of the technical staff from 1983 to 1989, where he worked on VLSI design and technologies, and InP-based opto-electronic IC technologies. In 1989, he joined Seoul National University as a Professor. In 2000, he started the Nano-Bioelectronics and Systems Research Center as Director, which is an ERC sponsored by the Korean Science and Engineering Foundation. His research is devoted to the design and fabrication of neural prostheses systems, development of nano and micro technologies for neural applications, and design of ASIC for neural signal processing.

Soon Joon Yoon received the B.S. degree from Yonsei University, Seoul, Korea, in 2006. He is currently working toward the M.S. degree with School of Electrical and Electronic Engineering, Yonsei University.

His primary research interest is in the area of highly sensitive nanowire-based surface plasmon resonance biosensors.

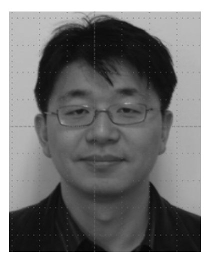

Donghyun Kim received the B.S. and M.S. degrees in electronics engineering from Seoul National University, Seoul, Korea, in 1993 and 1995, respectively, and the Ph.D. degree in electrical engineering from the Massachusetts Institute of Technology, Cambridge, MA, in 2001.

He was with Corning Inc., Corning, NY, and with Cornell University, Ithaca, NY, before he joined the School of Electrical Engineering, Yonsei University, in 2004. His current research interests are focused on biomedical applications of optics and optoelectonics including highly sensitive surface plasmon resonance, live-cell imaging, and *in vivo* optical imaging.